IMPACTS OF CENTER OF MASS SHIFTS ON MESSENGER SPACECRAFT OPERATIONS*

D. J. O'Shaughnessy, R. M. Vaughan and T. L. Chouinard III
The Johns Hopkins University Applied Physics Laboratory

D. E. Jaekle
PMD Technology

ABSTRACT

The MESSENGER (MErcury Surface, Space ENvironment, GEochemistry, and Ranging) has successfully completed its first three years of flight operations following launch on August 3, 2004. As part of NASA's Discovery Program, MESSENGER will observe Mercury during flybys in 2008 and 2009, as well as from orbit beginning in March 2011. This paper discusses the impact that center of mass (CM) location changes have had on many mission activities, particularly angular momentum management and maneuver execution. Momentum trends were altered significantly following the first deep-space maneuver, and these changes were related to a change in the CM. The CM location also impacts maneuver execution, and uncertainties in its location led to the significant direction errors experienced at trajectory correction maneuver 11. Because of the spacecraft sensitivity to CM location, efforts to estimate its position are important to momentum and maneuver prediction. This paper summarizes efforts to estimate the CM from flight data, as well as the operational strategy to handle CM uncertainties and their impact on momentum trends and maneuver execution accuracy.

INTRODUCTION

Flight operations are underway for the MESSENGER – MErcury Surface, Space ENvironment, GEochemistry, and Ranging – mission. As part of NASA's Discovery Program, MESSENGER will be the first spacecraft to observe the planet Mercury closely since the Mariner 10 flybys of the mid-1970s. The spacecraft was launched on August 3, 2004, and successfully completed its Earth flyby on August 2, 2005, and Venus flybys on October 24, 2006, and June 5, 2007. The spacecraft will make three Mercury flybys prior to orbiting Mercury for one Earth-year beginning in March 2011. The cruise phase of the mission has five large deterministic deep-space maneuvers (DSMs) that, coupled with the flybys, provide the necessary ΔV to target the spacecraft for its Mercury orbit insertion (MOI) burn in 2011. The Mercury flybys will assist in developing the focused science gathering for the year-long orbital portion of the mission (Ref. 1).

The spacecraft design (Refs. 2, 3) is driven by the thermal and radiation environment at Mercury. A large sunshade is used to protect most of the spacecraft systems from the heat and radiation of the Sun as shown in Figure 1. The shade must be kept between the Sun and the main body of the spacecraft whenever

* The work described in this paper was performed at the Johns Hopkins Applied Physics Laboratory, under contract (NAS5-97271) with the National Aeronautics and Space Administration, Discovery Program Office.

MESSENGER is within 0.85 AU of the Sun. The design of the sunshade allows for deviations of +/-10° from direct Sun pointing in rotations around the spacecraft *z*-axis, and +/-12° in rotations around the *x*-axis. This Sun keep-in (SKI) zone is a significant constraint to the attitude, which in turn impacts the science observation opportunities, maneuver design, and momentum accrual due to solar radiation pressure.

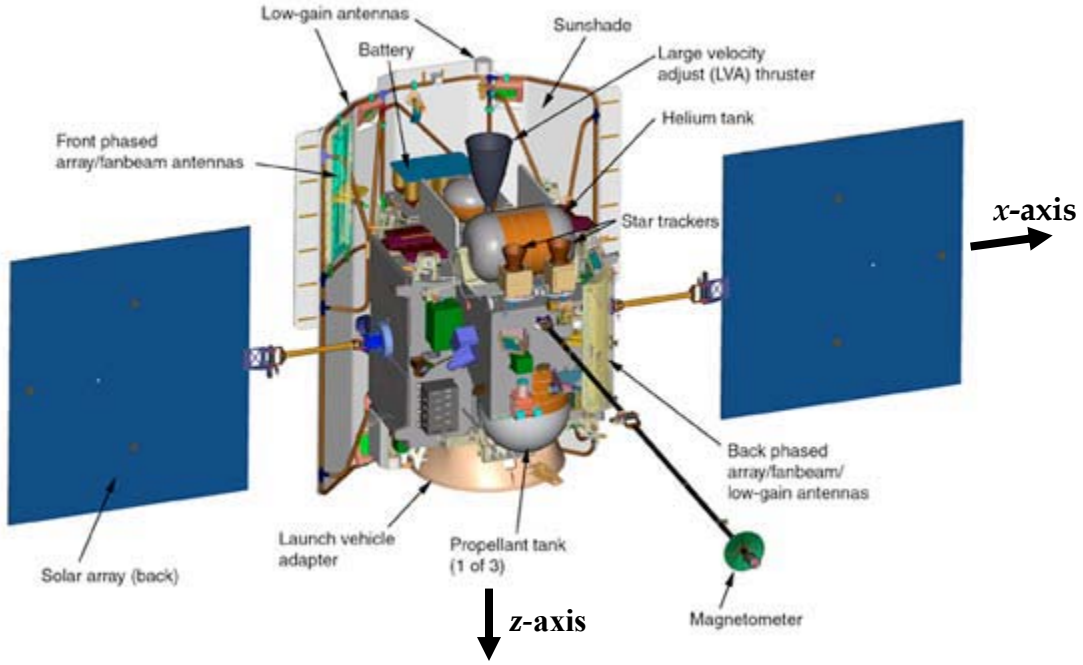

Figure 1. MESSENGER Spacecraft Components

The primary function of the MESSENGER Guidance and Control (G&C) System is to maintain spacecraft attitude for science and engineering activities and to execute propulsive maneuvers for momentum and trajectory control. The G&C system maintains a 3-axis stabilized spacecraft using reaction wheels as the primary actuators for attitude control. Star trackers and an inertial measurement unit containing four gyros provide knowledge of inertial attitude and rotation rates. Sun sensors are used to provide Sun-relative attitude knowledge as a backup to the inertial sensors for spacecraft safety.

The MESSENGER propulsion system has three primary functions: to impart ΔV during trajectory correction maneuvers (TCMs), off-loading reaction wheel momentum, and as a backup attitude control system in the event of multiple wheel failures. The system was designed and built by Aerojet and consists of four propellant tanks and 17 thrusters. The Large Velocity Adjust (LVA) thruster is the only bi-propellant engine on the spacecraft; it supplies 680 N of thrust, and its location is indicated in Figures 1 and 2. There are two sets of monopropellant thrusters, twelve 4.4-N thrusters and four 22-N thrusters, shown in Figure 2. Eight of the 4.4 N thrusters, designated A1-4 and B1-4, are used for small-ΔV burns orthogonal to the sunline, and they provide attitude control for all other maneuvers and during momentum dumps. The remaining four 4.4-N thrusters, designated S1-2 and P1-2, are used for small velocity changes in the sunward or anti-Sun direction. The four 22-N thrusters provide medium velocity changes orthogonal to the sunline, and also provide attitude control when using the LVA. The LVA provides the ΔV for large maneuvers, such as the five DSMs and the MOI burn. Three large propellant tanks are mounted along the spacecraft *y* axis, with the +*y* and –*y* tanks containing fuel, and the tank centered at the origin of the *xyz* coordinate frame contains the oxidizer, as seen in Figure 2. These three tanks are pressure regulated by a helium pressurization system. They contain two ring baffles each but do not have diaphragms, so the propellant is free to move within the tanks. All tanks are indicated in Figure 2. Because the tanks lack

diaphragms, the main tanks may be used only for maneuvers that have an acceleration directed in the +z direction, as the outlet of the tanks is located at the -z end. To ensure there is propellant settled at the outlet end of the tank, all burns using the main tanks must first conduct a short "settling burn" to drive the propellant to the outlet end of the tank. To fuel these settling burns, as well as any small ΔV in any direction other than +z, a fourth propellant tank, the auxiliary tank is used. This tank contains a diaphragm but is not pressure regulated, and due to its small volume, it must be refilled from the main fuel tanks periodically throughout the mission.

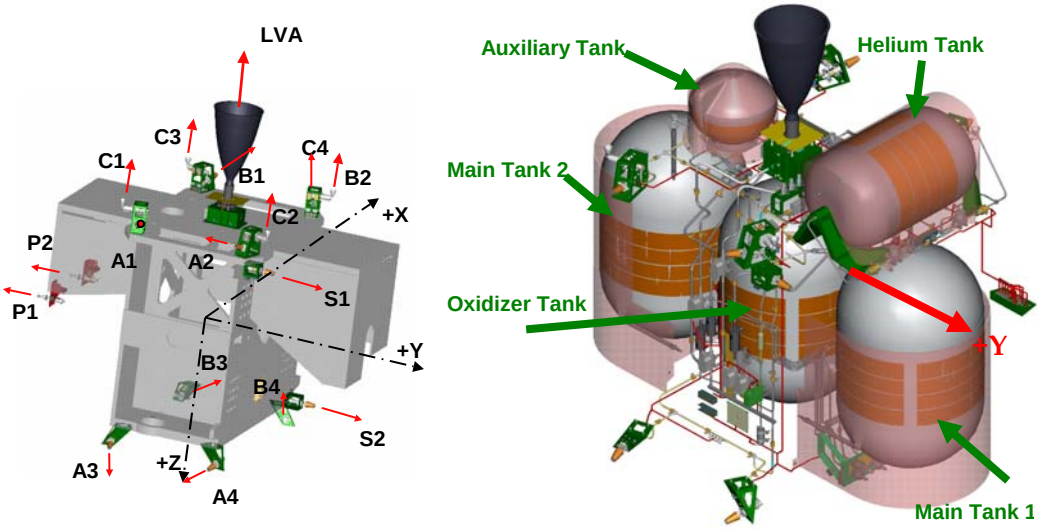

Figure 2. MESSENGER Thrust Directions and Tank Layout

The intricate trajectory design requires many TCMs to ensure precision targeting at the flybys and to maintain the science orbit at Mercury. The thrusters are positioned such that ΔV for these smaller maneuvers may be supplied in any Cartesian direction while simultaneously maintaining the SKI constraint. These thruster sets are oriented such that they provide efficient ΔV, however, their placement and alignment can simultaneously generate significant torque on the spacecraft when coupled with an unfavorable center of mass (CM) location. This torque from the thrusters supplying ΔV is (in general) counteracted with pulsing of the A and B thrusters to ensure a stable attitude, but this additional pulsing creates a perturbation on the imparted ΔV. The impact is most pronounced when using a pair of thrusters (like the S or P thrusters) for supplying ΔV, as was done at TCMs 5, 6, 11, and 13. This effect was the primary cause of significant direction errors on TCM-11. This paper will discuss the impact of CM location on the direction anomaly at TCM-11, as well as efforts to estimate the CM.

The MESSENGER spacecraft uses reaction wheels for attitude control, making momentum management an essential guidance and control task. Solar pressure acting on the sunshade and solar arrays is the main contribution to momentum accumulation. The time between active offloading of momentum using thrusters should be maximized to conserve propellant and minimize perturbations to the spacecraft's trajectory. The solar torque can be passively manipulated by changing the spacecraft's attitude and solar panel orientation. This passive momentum control technique has been used successfully since launch, but its relative effectiveness is dependent on the CM location. The solar torque experienced at a given sunshade orientation varies as the CM moves relative to the shade's center of pressure. Flight experiences with predicting momentum build-up due to solar torque and managing spacecraft attitude to control it are described in the next section. The largest changes in momentum build-up were observed after DSM 1 and TCM-10. A propellant motion analysis confirmed that shifts of the CM due to different locations of the

propellant masses in the main fuel tanks did occur as a result of executing these maneuvers. The implications of this analysis on future momentum management and maneuver execution are presented.

MOMENTUM TRENDING AND CM IMPACT

The use of solar torque for passive momentum control had been planned as part of the MESSENGER flight operations from the very early development stages (Ref. 4). Pre-launch momentum analyses primarily focused on the orbital phase since thruster momentum dumps will then be most disruptive to attempts to determine Mercury's gravity field. No specific analysis was performed to predict the frequency of thruster momentum dumps in the cruise phase, but there was a general desire to minimize thruster and propellant use. The cruise phase also provided an opportunity to try out the proposed momentum management techniques and verify the ground analyses. The spacecraft's attitude profile and panel angles could be optimized for momentum management while still maintaining high-gain antenna pointing at Earth and generating sufficient power from the arrays.

Models of solar torque had been developed for the sunshade and the solar panels since the spacecraft would be flying in the shade-to-Sun orientation for most of the mission. The shade and panels present regular, nearly uniform surfaces to the solar wind so that standard equations for solar pressure acting on a flat plate could be used (Ref. 5). The sunshade orientation relative to the Sun line and the location of its center of pressure, relative to the spacecraft's center of mass, determine the solar torques acting on the spacecraft's x- and z-axes. A change in Sun elevation angle, corresponding to a rotation about the spacecraft x-axis, results in a change in the x component of solar torque and system momentum. A change in Sun azimuth angle, corresponding to a rotation about the spacecraft z-axis, results in a change in the z-component of solar torque and system momentum. A solar torque about the spacecraft's y axis can be generated by rotating each solar panel by an equal angle, but in opposite directions, from a common base position. The x-axis momentum build-up was predicted to be larger than that of the y or z components, so changes in Sun elevation, or "tilts," of the sunshade were expected to be used most frequently for momentum control.

Power and thermal constraints dictated that the spacecraft should be oriented with its shade away from the Sun between launch and March 2005. The back of the spacecraft, with blankets covering its boxy structure, presents an irregular surface to the solar wind compared to the sunshade. A very crude model was developed for solar torque with the back of the spacecraft pointed toward the Sun, but it was not intended to be a highly accurate predictor of the momentum response to attitude changes. Given the short time that the spacecraft would be back-to-Sun and the numerous other check-out activities to be done at the beginning of the mission, no attempt was made to use spacecraft attitude for momentum control when the back of the spacecraft was toward the Sun. Experiments with passive momentum control were confined to changes in the solar panel angles to affect the y component of momentum. A short test was performed on 27 September 2004 where the panels were moved to positions that differed by 30°. An empirical fit of rate of change of y-axis momentum as a function of panel angle difference was made from flight telemetry. The resulting small (~2.7°) angle difference, needed to null out the rate of y-axis momentum change, was applied on October 8, 2004. Momentum dumps were combined with TCM-2 executed on September 24, 2004, and TCM-3 executed on November 18, 2004, to control overall system momentum magnitude.

The first opportunity to use a tilt of the sunshade for passive momentum control came after the first change to the shade-to-Sun orientation in March 2005. Flight telemetry with the spacecraft at the new orientation showed much larger than expected rates of momentum build up on the x and y axes. These rates did not match the prediction from the analytic model for solar torque from the sunshade and solar panels. A significant effort would have been needed to develop algorithms to estimate new values (or changes to the default values) for the complete ensemble of parameters in the solar torque models from

the flight data. However, there was an immediate need to determine the time frame when a thruster momentum dump might be needed. A simple two-stage approach was developed that could reliably predict the spacecraft momentum profile in the future. Given that torque is the time rate of change of momentum (Ref. 5), the effective solar torque on the three spacecraft axes could be derived from system momentum estimates in telemetry over several hours where the spacecraft stayed at the same attitude and panel positions. The analytic models showed a nearly linear relationship between Sun elevation and *x*-axis solar torque and between panel angle difference and *y*-axis solar torque. The slope and intercept of two lines defining the *x* and *y* torque were determined by combining the results of the torque fits from time periods where the spacecraft at different tilt angles and the panels at different offset positions. The linear equations for the solar torque could then be used to derive momentum changes over time. A simple integration scheme was developed to accumulate increments of momentum over specified time steps based on the expected Sun elevation and panel delta angles. The solar torques were applied in the spacecraft body frame, then converted to an incremental momentum change in the inertial frame and added to the inertial momentum at the start of the time step. Initial versions of this momentum integrator assumed that the spacecraft would remain at its downlink attitude at all times and only allowed changes in the tilt angle at the downlink attitude. This downlink attitude is defined such that the Earth in either the $+x$, $+y$ or $-x$, $-y$ quadrant of the x-y plane, and the Sun is within the SKI zone. Over time, the ability to model a wider range of spacecraft attitudes has been added. This integrator is being used to evaluate the effect of different solar array and body tilt angles in future periods and to recommend a strategy that will keep momentum magnitude at a low level where thruster dumps are not needed.

Three separate tilt changes were applied on March 30, March 31, and April 1, 2005. The tilt on March 30 placed the Sun at +20° elevation and the tilt on March 31 placed the Sun at -15° elevation. Both of these tests had been previously planned to evaluate thermal control strategies at the shade-to-Sun orientation. The tilt on April 1 placed the Sun at -5° elevation. The solar panels were simultaneously placed at angles offset by 2° in different directions from the nominal face-on to Sun angle for this attitude. This test was added to get additional data for the solar torque and momentum predictor models. Data from these periods were used to determine values for the tilt and panel offset angles that would prevent having to execute a thruster dump. On April 5, the downlink attitude was changed to place the Sun at -7.05° elevation and the panels were commanded to angular positions that differed by 2.34°, each 1.17° away from the face-on to Sun position in different directions. Momentum estimates from telemetry over the next few weeks verified that the simple tools were accurately predicting momentum trends. Another tilt change to -9.175° was made on May 24, 2005, to further lower the momentum magnitude prior to returning to a back-to-Sun attitude on June 14, 2005. The panels were moved to positions consistent with this new tilt, but still with an offset of 2.34° between them.

The spacecraft returned to the shade-to-Sun orientation on September 7, 2005. The same tilt with the Sun at -9.175° elevation and panel offset angle of 2.34° were applied as had been used in May and June. This was based on the solar torque solutions derived from the March and April telemetry. The rate of change of momentum in September was somewhat higher than predicted. This difference between the model prediction and flight momentum estimates was the first indication that a CM shift may have occurred. New solutions for the linear relationship between *x* torque and tilt angle were made from the latest telemetry allowing the model to better predict momentum trends leading up to DSM-1 in December. The "tilt" angle was changed from -9.175° to -5° on October 20, 2005. The same relative panel angle difference was maintained. Another change to put the Sun at -4° elevation was made on October 28, 2005.

While the relationship between *x* solar torque and sunshade tilt angle had changed from the initial solution by fall of 2005, the change was not dramatic. It was still possible to obtain both positive and negative *x* torques with tilt angles within the Sun keep-in bounds (-12° to +12°). A far more dramatic change occurred with the execution of DSM-1 on December 12, 2005. Figure 3 shows the rate of change of *x* momentum before and after DSM-1. The strategy for the tilt angle after DSM-1 and into 2006 has

been based on the prior trends and the spacecraft had been returned to its -4° tilt after the maneuver. The first few days of telemetry after the burn showed a significant change in the momentum trend, with an order of magnitude increase in the rate of change of momentum about the *x* axis. The shift in the line for *x* torque was large enough that only negative *x* torque would be possible at allowable tilts. Any new tilt angle would only slow the rate of increase of *x* momentum, not reverse its direction. A thruster momentum dump would ultimately be needed. Fits of solar torque to tilt angle were refined from additional telemetry and a new strategy for momentum control was developed in the week following DSM-1. New tilt angles were found that allowed the execution of the first thruster momentum dump to be delayed into January 2006, giving the operations team time to prepare the necessary command sequences. After taking into account the redistribution of momentum components resulting from a 180° turn to switch antenna sets on December 22, the tilt angle was changed to put the Sun at -12° elevation on December 15, then changed to 0° tilt on December 20 and restored to -12° following the rotation to switch antennas on December 22. The tilt angle of -12° minimized the rate of change of *x* momentum while staying within the Sun keep-in bounds. The first thruster dump executed successfully on January 10, 2006, and set the momentum at a value that would not require further dumps until TCM-10, scheduled for February 22, 2006.

The momentum target selected for TCM-10 and the tilt and panel offset angles to be applied after it were based on the solar torques derived from post-DSM-1 telemetry. Once again, another large shift in the *x* momentum build-up rate was seen in telemetry after TCM-10 as shown in Figure 3. This time the data indicated that the line giving *x* torque as a function of tilt angle had readjusted to a more favorable location where both positive and negative torques could be obtained with tilts within the SKI bounds. A new fit for *x* solar torque was derived and used to update predicted momentum magnitude leading up to a return to the back-to-Sun orientation on March 8, 2006. Two changes based on this new predict were made in the tilt angle immediately after TCM-10. The Sun elevation was changed to -7.4° on February 23 and then to +0.24° elevation on February 25.

The change in momentum trending after DSM-1 had not been expected. Pre-launch estimates of the spacecraft CM after the DSMs had assumed that the propellant mass in the main tanks would return to a nearly central location so that the CM shift in the *z* direction would be small. The large change in momentum build-up indicated that the actual CM location was probably closer to the predicted CM during LVA firing when the propellant was held over the outlets at the –*z* end of the tanks. There was no question that the propellant masses would move during DSM-1 given the large ΔV of 315 m/s and consumption of over 100 kg of propellant, but the assumption of restorative motion after the LVA stopped firing needed to be reexamined. It was more surprising that propellant motion would have occurred for the relatively small ΔV of 1.41 m/s applied at TCM-10 using the B thrusters. With two propulsive maneuvers resulting in significant changes in momentum trends, the project initiated a propellant motion analysis to determine the most likely location of the propellant masses after TCMs up to TCM-10 and predict the likely location after future maneuvers using the different thruster sets. Of particular importance is which thruster firings could lead to a shift in *x* torque vs. tilt angle that would prevent effective control with tilts in the allowable range similar to the situation after DSM-1.

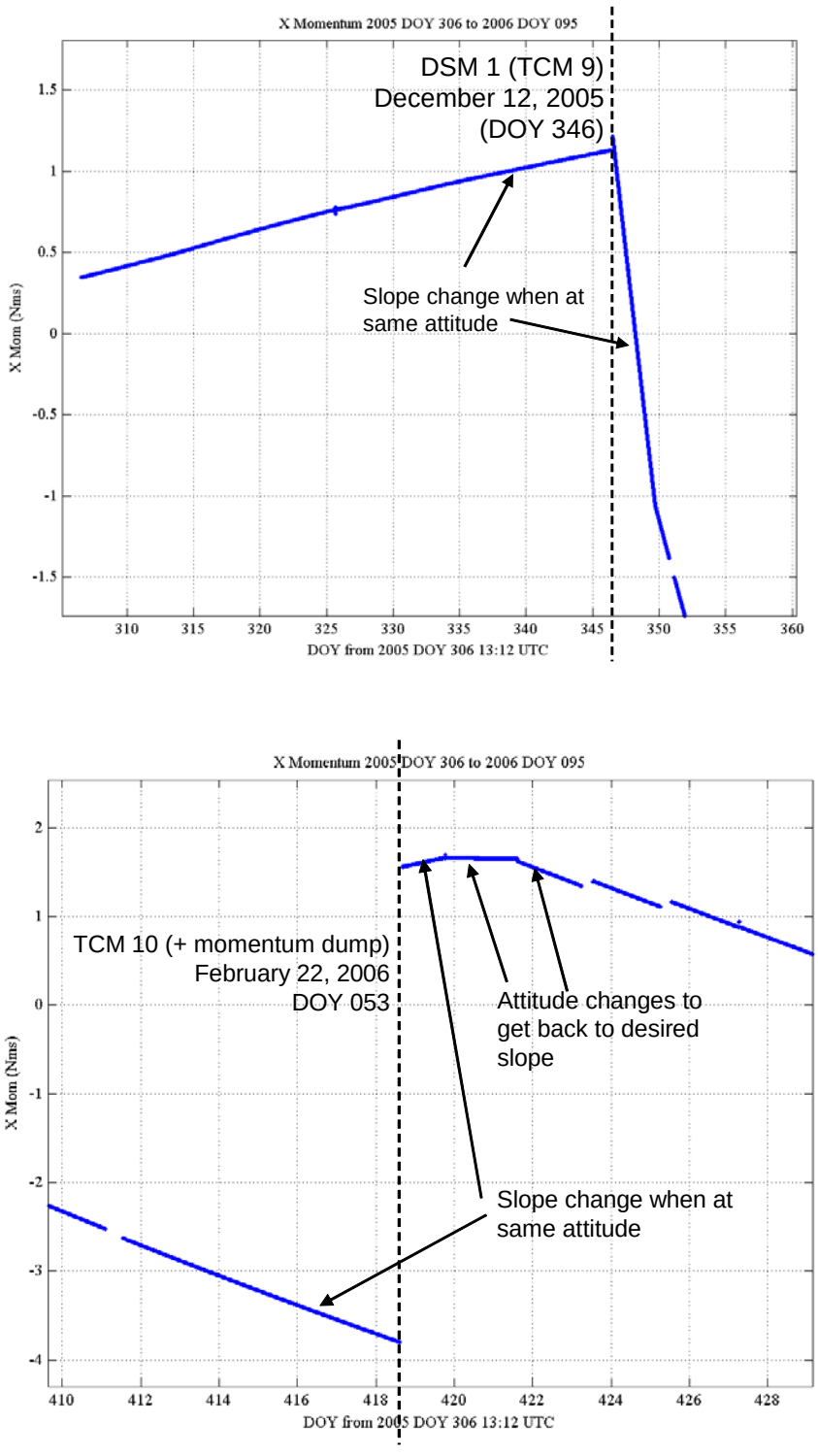

Figure 3. MESSENGER x Momentum after DSM-1 and TCM-10

PROPELLANT MOTION WITH TCMS AND MANEUVER PLANNING

The propellant motion studies performed after TCM-10 used computational fluid dynamics methods to model the motion of the fuel and oxidizer masses in the three main tanks. Results showed that the surface tension dominates the shape and movement of the fluid masses and confirmed that the propellant will remain in the end-of-burn configuration until the next thruster firing. Angular acceleration due to wheel slews and linear acceleration due to solar pressure are not sufficient to change the shape of the propellant masses. Detailed simulations were run to determine the CM of each propellant mass before and after DSM-1 and after the remaining future DSMs. The analysis showed that any LVA firing longer than 10 s moves the propellant masses directly up against the tank outlets. Therefore, all DSMs will leave the propellant CM centered axially in the tanks, with the *z* component of the CM slowly becoming more negative (moving toward the tank outlet). The worst-case *z* axis CM offset will occur some time into the MOI maneuver. If the DSMs continue to be executed solely using C thrusters and the LVA, the momentum trends will become difficult to manage using only solar torque effects and the effectiveness of this passive control will degrade after each future DSM. A similar result was predicted for any C thruster firing longer than 35 s, and it is expected that long firings of A and B thruster combinations with a net +z thrust will also move the propellant masses in the same direction. With nothing to move the masses after thruster firing is stopped, more frequent thruster momentum dumps can be expected after any sufficiently long burn with only axial thrust.

Another detailed simulation was run to determine the propellant motion during and CM location after TCM-10. Results showed that the CM did shift in the +z direction (away from the tank outlets, back toward the center of the tanks) under the influence of the lateral acceleration from the B thrusters. TCM-10 fired the B thrusters for $-x$ acceleration over a period of 118 s, which was long enough to move the propellant masses to a more favorable position reversing the adverse momentum trending seen following DSM-1. It is expected that any sufficiently long duration of lateral (*x*- or *y*-axis) acceleration from A, S, or P thrusters will have a similar effect. This means that the adverse CM movement from axial thrust can be countered by following it by a period of lateral thrust.

Although cost constraints prohibit running a set of fluid dynamics simulations for every TCM, some general guidelines from the analysis have been and will continue to be applied to future operations. The first example was the execution of TCM-11 in September 2006. The ΔV vector for TCM-11 had to be broken into components to keep the spacecraft attitude within the SKI zone. Initial plans called for firing the S thrusters for lateral thrust followed by firing of the C thrusters for axial thrust. Either order of S and C firings in the two directions would sum to the same resultant vector, but they would have very different ending CM locations. To minimize the effect on post-burn momentum trends leading into the first solar conjunction, the order of thruster firing was reversed with axial thrust preceding the lateral thrust. This same strategy can be applied to any large TCM or a DSM. There will be a penalty in propellant usage as the component burn is less efficient than thrusting directly in the target direction. Also, a component vector set that is closest to the target direction while still in the SKI bounds may have to be altered so that the lateral component is of sufficient duration. The number of thruster momentum dumps to be planned and executed after a large TCM or DSM can be lowered with sufficient lateral thrusting after a large axial thrust. While it would take a very large number of momentum dumps to equal the propellant mass needed for sufficient lateral thrust to move the propellant masses, the benefit of not adding more activities to an already busy mission timeline may outweigh the decrease in the margin in the ΔV budget. TCM-13 executed in December 2006 followed this strategy, implementing its total ΔV of 25.63 m/s with lateral thrust components using the P thrusters before and after the axial component using the LVA. A lateral component is also planned as the last segment of DSM-2 to be executed in October 2007. The operations team is also working to streamline the procedures for executing thruster momentum dumps to make their execution less labor intensive.

TCM-11

TCM-11 was performed on September 12, 2006, and was the first two-component maneuver executed by MESSENGER. This component burn used two consecutive sets of thruster firings to achieve the desired target ΔV. This was necessary to maintain spacecraft attitude within the SKI zone. There were no problems with G&C commanding, propulsion system configuration, or maneuver performance when executing the first part of TCM-11. The first component used the 22-N C thrusters for ΔV in the +*z* direction with a subset of the 4.4-N A and B thrusters pulsing as needed for attitude control. Thrusters fired for 54 s to reach the target ΔV magnitude of 0.830 m/s. The on-board estimate of the actual ΔV magnitude from accelerometer data was 0.840 m/s or 1.2% "over burn" with a direction error of 1.2°; ground processing of the high-rate data taken during the burn confirmed the onboard estimates. There were no problems with G&C commanding or propulsion system configuration during component 2 of TCM-11; however, the maneuver direction performance was anomalous. The second component used the 4.4-N S thrusters for ΔV in the –*y* direction with a different subset of the 4.4-N A- and B thrusters pulsing as needed for attitude control. A momentum dump was combined with this component to reduce system momentum in advance of the 47-day solar conjunction following the burn. Thrusters fired for 202 s to reach the target ΔV of 1.46 m/s and continued to fire up to the 235 s time-out duration to maintain the momentum target. The on-board estimate of the actual ΔV magnitude from accelerometer data was 1.461 m/s or 0.1% "over burn" with a direction error of 11.2°; ground processing of the accelerometer data and navigational data confirmed the large direction error.

The larger than expected direction error experienced at TCM-11 was the result of several conditions, one of which was the maneuver design. As mentioned in the prior section, this maneuver was chosen to be implemented as a component burn since the desired ΔV was oriented such that the Sun keep-in limits prevented achieving the target ΔV direction with a single thruster set. A portion of the burn was along the spacecraft-Sun line, so that required the use of the S thrusters. The remainder of the desired ΔV was directed orthogonal to the spacecraft-Sun line, so there were three thruster sets that could be used, the A, B, or C thrusters. Because of problems experienced at TCM-10 with thruster plume impingement effects on the solar arrays, the C thrusters were selected as the plume impingement problem impacts both the A and B thruster sets. Furthermore, the C thrusters have a higher I_{sp} than the S thrusters, so the geometry for the maneuver was chosen such that the C thruster component would be maximized, thereby saving fuel. The order of the components was chosen to minimize the momentum trends during the ensuing conjunction, without regard to the impact that might have on the execution of the burn. This design put the spacecraft very near the 12° SKI constraint limit for the second component. Because of the proximity to the SKI constraint limit, the decision was made to tighten the attitude flexibility given to the guidance algorithm for the maneuver. The guidance attempts to make adjustments to the commanded attitude so that errors in the ΔV are removed during the burn. Normally, the guidance is allowed to steer the spacecraft by 2 to 6°, depending on the burn, but for this burn the limit was reduced to 0.5° to ensure that the SKI limits would not be violated. By restricting the guidance in this way, the spacecraft was unable to turn to compensate for the direction errors, in favor of ensuring that the spacecraft remained sun-safe.

A second contributor to the direction error at TCM-11 was the decision not to off-pulse the S thrusters for attitude control. It was desirable to fire the thrusters at 100% duty cycle, since that produced reliable burn duration; whereas off-pulsing an unknown amount (in response to the CM location) produced a wider distribution of burn times. A deterministic burn duration was desirable as TCM-11 was to be paired with a momentum dump to reduce momentum for the upcoming flyby and ensuing conjunction. When pairing a maneuver with a momentum dump, they will ideally end at the same time. If the momentum dump ends prior to the burn, the wheels will spin down from their desired targets until the burn completes, negating much of the targeted momentum. Conversely, if the burn ends before the dump, the thruster pulses required to dump momentum after the burn completes are a perturbation on the desired ΔV. Firing the S thrusters at 100% duty cycle allowed the timing of the burn and the dump to be more

closely coordinated. Further, pre-burn simulations revealed that maneuver performance was similar for cases run with off-pulsing and burns where the S thrusters were fired at 100% duty cycle.

Although the first component of TCM-11 executed nominally, it did have an adverse impact on the CM location. Because the first component was a Mode 2 burn, it used the fuel supplied from the main fuel tanks, which required a settling burn to be performed in advance of firing the C thrusters. This settling burn, coupled with the direction of the C thrusters, drives the propellant toward the –*z* end of the tanks, thereby moving the CM down from the prior configuration. This motion of the CM in the -*z* direction is benign for this maneuver, as the torque generated by the C thrusters is independent of *z*-axis CM location. Further, the C thrusters bracket the CM location in the *x*-*y* plane, which allows the C thrusters to completely handle torque perturbations due to CM location by off-pulsing. This is important because the vast majority of the attitude control torque required during a burn is due to the torques resulting from firing the main thrusters used to supply ΔV. By handling these torques with the thrusters used to supply ΔV, the attitude control does not perturb the achieved ΔV. This is only true for thrusters that have the same thrust direction and completely bracket the CM in a plane orthogonal to their thrust axis, which for MESSENGER, includes only burns on the C thrusters. If the CM in the *x*-*y* plane were to move outside the physical location of the C thrusters in that plane, then torques resulting from that CM location could not be handled by off-pulsing the C thrusters. This condition is not expected to occur on MESSENGER since the location of the C thrusters relative to the geometric center of the spacecraft is greater then 44 cm in both *x* and *y*, and the expected CM location should remain within 5 cm of the center of the spacecraft in both *y* and *y*. In fact, the CM location in *x* and *y* must be maintained more tightly (to within ~1 cm of the origin of the spacecraft coordinate frame), or during LVA burns torques from firing the main engine could quickly overcome the control authority of the C thrusters, resulting in a loss of attitude control.

The second component of TCM-11 was impacted by the CM motion experienced during the first component. There are only two S thrusters, and as such they can only control those CM offsets that are on a line between the thrusters. The S thrusters produce thrust in the –y direction, so they are not sensitive to shifts or uncertainty in the CM along the *y*-axis. However, *x* and *z* shifts will result in *z* and *x* torques, respectively. The S thrusters have limited control authority over this torque via off-pulsing. In the case of TCM-11, the S thrusters had no control authority, since the decision was made to fire them at 100% duty cycle. This thruster strategy produces a bias torque for any CM that is not at the midpoint of the line between the two S thrusters. Of course, the CM did not lie at this location for TCM-11 and a bias torque resulted from the ΔV thrusters. For attitude control, this torque had to be counteracted by the other thrusters in use. In the case of TCM-11, these supplemental attitude control thrusters were the A and B clusters, which had thrust directions that were nearly orthogonal to the desired ΔV. The thrusters are mounted such that four thrusters can be fired simultaneously to generate a pure couple; however, the thruster control law does not fire the thrusters in this way. Each thruster has its own phase plane, and the control logic makes a decision whether or not to fire the thruster based on the attitude and rate errors projected onto the torque axis for a particular thruster. This law is fuel efficient and fault tolerant but rarely produces pure torques. In the case of TCM-11, these attitude control pulses resulted in a bias force in the +x direction. This force bias is difficult to discern in the noisy acceleration data but is readily apparent in the linear growth in the *x*-axis ΔV, as shown in Figure 4.

The attitude control pulsing that produced the accumulated ΔV profile, shown in Figure 4, was unexpected. The expectation was that all of the ΔV in the body frame would be aligned with the –*y*-axis. The linear growth in *x* was due to attitude control firing and this produced the significant direction error. The pattern of thruster firings for TCM-11 was also different than predicted by the pre-burn Monte Carlo simulations. These Monte Carlo simulations produced the *a priori* thruster duty cycles tabulated in Table 1. Table 1 also shows the true values based on the flight telemetry. These values show significant differences from the Monte Carlo predictions. The discrepancies are especially pronounced on thrusters A1, A4, B1, and B4. Analysis of the thruster pulsing seen in the flight data led to a simple estimate of the

center of mass based on conservation of angular momentum during the burn. Since the attitude for the burn was nearly constant, the thruster activity should produce zero net torque on the spacecraft. By guessing a CM, the theoretical torque (based on thruster performance data and known thruster locations/alignments) could be calculated. With the aid of a simple numerical optimization routine, the CM was found that minimized the torque during the maneuver. This CM is tabulated in Table 1 as the *a posteriori* CM. Using that information, an additional simulation of TCM-11 was run which produced duty cycles for each thruster that match very closely with the flight telemetry, as shown in Table 1.

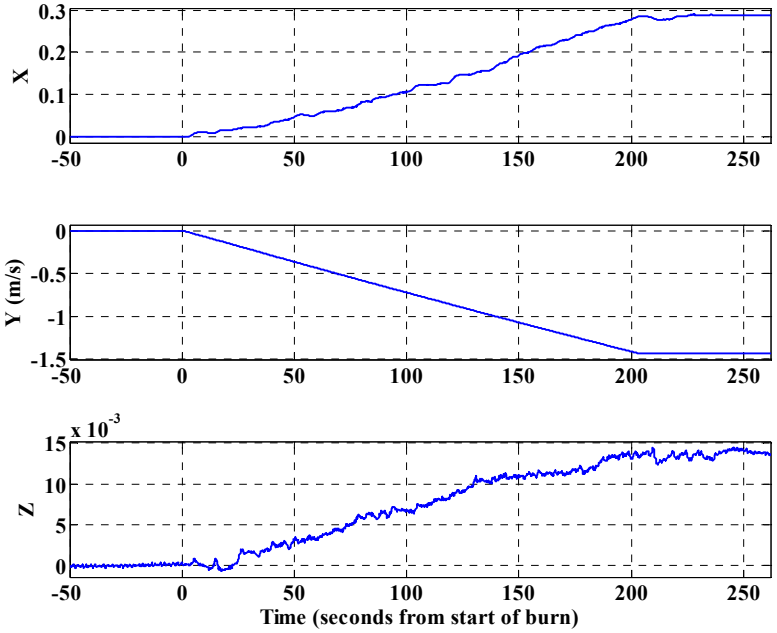

Figure 4. TCM-11 Component 2 Accumulated ΔV in Spacecraft Body Coordinates

Table 1. TCM-11 Component 2 Thruster Duty Cycles

	Thruster Duty Cycle (%)								Spacecraft CM (m)
	A1	A2	A3	A4	B1	B2	B3	B4	
***a priori* Simulation**	23.5	3.9	5.4	20	24	5.4	4.9	21.3	[0 -0.004 -0.03]
Flight Telemetry	35.9	0.1	5.2	30.7	11.7	5.3	0.1	15.1	Unknown
***a posteriori* Simulation**	36.1	0.1	5.1	32.7	9.5	4.5	0.1	12	[-0.03 -0.005 -0.066]

The reaction torque produced by pulsing the thrusters in the pattern shown in Table 1 demonstrates that the torque produced by firing the S thrusters was different from that predicted by ground models. The simple preliminary analysis has been based on the assumption that all of this difference could be explained by uncertainty in the CM, but that is not the only possible explanation. There are several possible modeling uncertainties that could explain this difference. These uncertainties include thruster misalignments, thruster magnitude performance, or plume impingement effects. While it is very likely

that all these effects are present to some degree, the errors in the Monte Carlo predictions appear to be dominated by a mis-modeled CM. That the simulated performance closely matches the flight performance with only a CM change is strong evidence to suggest that the CM uncertainty is the dominant effect. This demonstrates the need to have a reasonable estimate of the CM prior to any maneuver if the team is to reliably predict the outcome with ground simulations. This is especially true for burns that use only two thrusters for ΔV. Efforts to formalize the estimation of the CM during thrusting events are presented later in this paper.

As seen at TCM-11, the CM has a large impact on the direction errors of any maneuvers using two thrusters for ΔV. In addition to TCM-11, other maneuvers that used two thrusters to supply ΔV included TCMs 5, 6, and 13. The S thrusters were used for TCM-5, and the P thrusters were used for TCMs 6 and 13. TCM-5 did not have the large angle errors seen at TCM-11 as all three of the conditions that led to this anomaly were not present. First, the S thrusters were off-pulsed to help control the attitude. Second, the burn attitude was centered in the SKI zone, and the guidance was allowed to steer the attitude to remove a larger portion of the direction error. Lastly, and most importantly, TCM-5 was prior to the first DSM, so the tank fill levels were closer to full, which helped move the *z*-axis component of the CM closer to the spacecraft coordinate frame origin. These three factors helped keep the angle errors on TCM-5 to 0.4º. P thruster burns experience similar effects as TCM-11, but the intersection of the plane containing their thrust vectors with the *z* axis is somewhat closer to the CM experienced on those burns. This minimized the torque produced by those thrusters on TCMs 6 and 13 and led to direction errors on those burns of 4.5º and 1.5º, respectively.

CM LIMITS ANALYSIS

With the burn and momentum sensitivities to the CM position, limits on the CM location in the spacecraft body frame are important to quantify. By understanding the parameters that impact the motion of the CM, appropriate limits can be set during ground simulations to allow better prediction of spacecraft behavior. There are two articulated devices that can have a minor impact on the spacecraft CM. The Mercury Dual Imaging System (MDIS) instrument contains two cameras mounted on a scan platform (Ref. 2). The position of the scan platform will have a small impact on the CM, as the mass of the instrument is small relative to the spacecraft, and the motion of the instrument in the spacecraft body frame is also small. Because the mass and range of motion of the camera are small, this motion is negligible. The solar arrays are also articulated, but since they are assumed to rotate about an axis that passes through their mass center, there is no impact on the overall CM. This fixes the CM of the dry mass, and the pre-launch estimates for this are shown in Table 2.

At launch, the MESSENGER propellant mass fraction was 54%, so the propellant location strongly influences the CM. The main fuel tanks and oxidizer tank do not contain diaphragms, so the propellant is free to move within each tank. The shape and location of the propellant in each tank introduces the largest uncertainty in determining the CM. Of course, the CM depends not only on the shape of the propellant in the tank, but also the mass, or fill level of the tanks. The CM can easily be computed for several worst-case positions and for the worst-case fill-levels for each tank. This defines an envelope for the expected CM location. In the case where all the propellant is settled at the outlet end of the tank, and the auxiliary tank is full, the CM change will have a large –*z* value. Conversely, when the propellant in the main fuel/oxidizer tanks is pushed to the +*z* end and the auxiliary tank is nearly empty (this tank is never fully drained), this creates a worst-case scenario for a +z CM offset. Using similar arguments for worst-case locations on the *x*- and *y*- axes results in the numbers shown in Table 2. This analysis is based on the assumption that the fill level of each main propellant tank is the same. If there is an imbalance in the fuel levels in these tanks, the CM in the *y* direction can vary by much more than the numbers shown in Table 2. Careful analysis and planning by the MESSENGER propulsion team is done to ensure that the fuel masses in these tanks remain within a few kilograms of one another. Uncertainty estimates for all of the tabulated values have not been computed, but they are assumed to be small. The intent of this analysis

was to produce approximate bounds for use in future Monte Carlo testing and as a benchmark for comparison with attempts to estimate the spacecraft CM.

Table 2. MESSENGER Center of Mass Bounds in Spacecraft Body Coordinates

	x-axis location (m)	*y*-axis location (m)	*z*-axis location (m)
Dry	0	-0.008	-0.055
Lower Limit	-0.052	-0.051	-0.131
Upper Limit	0.052	0.037	0.047

CM ESTIMATION FROM FLUID DYNAMICS ANALYSIS AND MESSENGER TELEMETRY

The momentum trending and maneuver performance for MESSENGER are strongly influenced by the CM. It is of interest to the G&C team to produce better, more reliable estimates of the CM than the pre-launch information supplied based on the computer-aided design models. There is a great deal of telemetry that can be used to infer dynamic modeling parameters. Thruster command data coupled with gyro and accelerometer data can be used to estimate the CM during burns. Some preliminary attempts have been made to investigate estimation of the CM among other dynamic parameters via methods described elsewhere (Refs. 6-8). This is a particularly difficult problem for MESSENGER, as the thruster forces and torques for the A and B clusters are not well known. The alignments and performance of these thrusters is well known, but they are subject to plume impingement on the solar arrays, which can drastically alter the resultant forces and torques. Although the impingement is not well characterized, there is evidence from several MESSENGER TCMs to suggest the effect is on the order of 10-20% in force. Ignoring an effect of this order of magnitude invalidates the model, and leads to erroneous or nonsensical results. So, impingement modeling must be included in any attempt to estimate dynamic parameters when thrusting is involved. Previous methods (Ref. 6) can be easily modified to account for uncertainties in the force and torque of a thruster, but this increases the number of unknowns dramatically, and it is unlikely that all of the parameters of interest are observable.

Since the CM remains unchanged between thruster events, CM estimates can be made based on trends in the momentum data between burns. This is a more promising route, as this eliminates the uncertainty in the propulsion system model. Pursuing this approach requires good estimates of the wheel alignments and inertias and the spacecraft inertias. In general, the information on these quantities is reliable, although the spacecraft inertia properties are likely the least reliable. There are many methods to estimate the inertia tensor (refs. 6-8), and this can be solved independently from finding the CM.

Using the momentum trends to estimate the CM requires careful modeling of the solar radiation pressure, as this technique involves a fit of torque due to solar radiation pressure to observed trends in the spacecraft system momentum. Solar pressure models for MESSENGER were developed prior to launch for use in the high-fidelity dynamic simulations to allow study of the momentum trends during the orbital phase of the mission (Ref. 4). The plate model developed for momentum modeling can be used in a least-squares estimator of the CM. This method has been implemented, and using the telemetry from normal flight operations, the CM estimate for July 2007 was created. These results are shown in Figure 5. It is obvious that the *y*-axis estimate is poorly known, as the solar radiation pressure force is nearly all directed along the *y*-axis, making the CM component in *y* difficult to observe. The locations in *x* and *z* are more readily seen and are reasonable values, based on the CM limits analysis previously discussed. This preliminary estimate appears reasonable and consistent with recent burn performance as well. There is still significant uncertainty in these estimates, as general flight operations do not satisfy the persistency of excitation condition necessary for reliable convergence. Effort is underway to design a simple maneuver that would allow reliable CM determination using the solar torque.

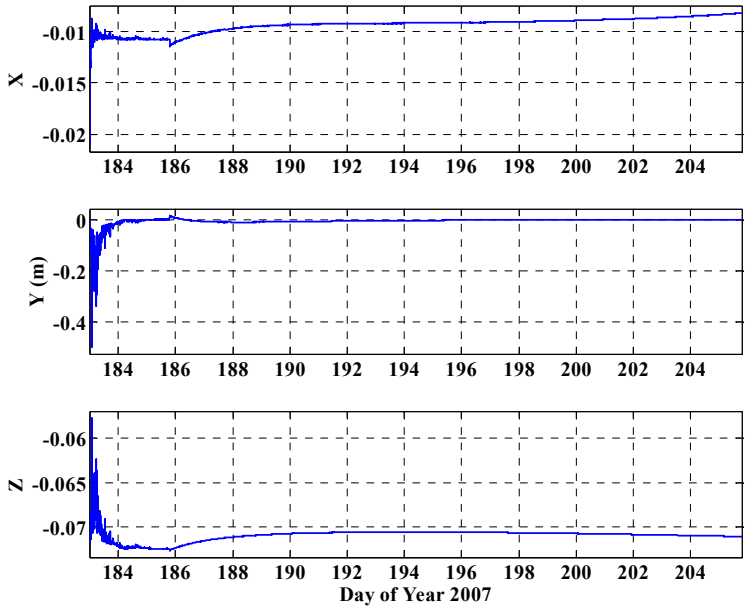

Figure 5. Center of Mass Estimate using July 2007 Momentum Telemetry

CONCLUSION

The CM location has a large impact on MESSENGER operations. It has been shown to drastically alter the momentum trends, impact the maneuver accuracy, and force the Operations Team to modify mission plans to account for these effects. There has been a great deal of work aimed at understanding the impact of the CM on mission performance, as well as how it will trend in the future. The G&C team is actively working on strategies to estimate the CM based on flight telemetry, in order to better plan and predict future events.

REFERENCES

1. S. C. Solomon et al., "The MESSENGER Mission to Mercury: Scientific Objectives and Implementation," Planetary and Space Science, Vol. 46, Issues 14-15, pp. 1445-1465, December 2001.

2. R. E. Gold et al., "The MESSENGER Mission to Mercury: Scientific Payload," Planetary and Space Science, Vol. 46, Issues 14-15, pp. 1467-1479, December 2001.

3. A. G. Santo et al., "The MESSENGER Mission to Mercury: Spacecraft and Mission Design," Planetary and Space Science, Vol. 46, Issues 14-15, pp. 1481-1500, December 2001.

4. R. M. Vaughan et al., "Momentum Management for the MESSENGER Mission," AAS/AIAA Astrodynamics Specialists Conference, Paper AAS 01-380, 22 pp., Quebec City, Quebec, Canada, July 30-August 2, 2001.

5. J. R. Wertz, *Spacecraft Attitude Determination and Control*, D. Reidel Publishing Co., Dordrecht, Holland, 1978.

6. E. Wilson et al., "Motion-Based Mass- and Thruster-Property Identification for Thruster-Controlled Spacecraft," Proceedings of the 2005 AIAA Infotech@Aerospace Conference, Arlington, VA, September 2005.

7. E. V. Bergmann et al., "Mass Property Estimation for Control of Asymmetrical Satellites," Journal of Guidance, Control and Dynamics, Vol. 10, No. 5, pp. 483-491, September 1987.

8. R. Reynolds, "Linear Recursive Inertia Estimator," 2005 Flight Mechanics Symposium, Greenbelt, MD, October 2005.